International Journal of Industrial Chemistry (2019) 10:225–236
https://doi.org/10.1007/s40090-019-0186-3

RESEARCH

Synthesis of TiO_2/nZVI nanocomposite for nitrate removal from aqueous solution

Zahra Hejri[1] · Mehri Hejri[1] · Maryam Omidvar[1] · Sadjad Morshedi[1]

Received: 31 August 2018 / Accepted: 4 June 2019 / Published online: 21 June 2019
© The Author(s) 2019

Abstract

To develop a new adsorbent for removal of nitrate and to enhance the adsorbent separation from aqueous solution, surface modification of titanium dioxide nanoparticles with nano-zero-valent iron (nZVI) was performed through chemical coprecipitation of magnetic nanoparticles on TiO_2 surface. Morphological, structural and magnetic properties of modified adsorbents (TiO_2/nZVI) were characterized by scanning electron microscopy (SEM), transmission electron microscopy (TEM), X-ray diffraction (XRD), Fourier transform infrared radiation (FTIR) and vibrating sample magnetometer (VSM). To determine the ionic strength effect and optimal removal conditions, the effect of contact time (60–210 min), pH (4–10) and adsorbent dosage (0.5–1.5 g/L) on adsorption efficiency were studied, using response surface method. Obtained results showed that the nitrate removal efficiency decreased with increasing ionic strength. The TiO_2/nZVI nanocomposites exhibited a ferromagnetic behavior and its saturation magnetization was 795.28 memu/g. The maximum nitrate removal (98.226%) achieved by modified TiO_2 was about 14.65% higher than the unmodified nanoparticles. The optimized adsorption parameters were: adsorbent dosage 0.982 g/L, pH 4.185 and the contact time 150.091 min.

Keywords Titanium dioxide · nZVI · Nitrate · Aqueous solution · Adsorption

Introduction

Nitrate is often found in drinking water because of human activities such as excessive utilization of chemical fertilizers, inappropriate disposal of industrial, human and animal wastes, etc. Nitrogen is converted to nitrate in the soil and since nitrate is dissolvable in water, it enters groundwater and eventually drinking water through the rain [1]. Increasing nitrate in drinking water has two adverse health effects: induction of blue-baby syndrome or methemoglobinemia, especially in infants, and the formation of carcinogenic nitrosamines [2].

✉ Zahra Hejri
zahrahejri@iauq.ac.ir

Mehri Hejri
mehri.hejri@yahoo.com

Maryam Omidvar
maryam_omidwar@yahoo.com

Sadjad Morshedi
sajjadmorshedi@yahoo.com

[1] Department of Chemical Engineering, Quchan Branch, Islamic Azad University, Quchan 94791-76135, Iran

Conventional nitrate removal technologies including ion exchange, reverse osmosis, electrodialysis, biological and chemical denitrification, are often costly and complex with low efficiency and sub-products [2–5]. Adsorption has been proposed as an attractive technology for removal of different pollutants from water due to its process simplicity, selectivity and reusability of the adsorbent, low cost and environment-friendly nature [6–14]. Khezri et al. [15] investigated the adsorption of nitrate anions from aqueous solutions on ammonium-functionalized magnetic mesoporous silica. The removal efficiency of NO_3^- from solution was around 86.24% by the constructed adsorbent under the optimal experimental conditions. Nowadays, nano-adsorbents are widely used to efficiently eliminate the pollutants from water due to high surface-to-volume ratio, easy synthesis and rapid sorption [3, 16]. Bhatnagar et al. [2] have investigated the removal of nitrate from aqueous solution using alumina nanoparticles and achieved the maximum absorption capacity of 4 mg/g at 25 ± 2 °C and pH 4.4. Farasati et al. [17] eliminated nitrate from contaminated waters using anion exchanger Phragmites australis nanoparticles. The highest adsorption rate was obtained at pH 6 using 0.3 mg/L adsorbent. Zhao et al. [13] reviewed the recent

works on the preparation of polymer composites and their application in the efficient removal of heavy metal ions from aqueous solutions under different conditions. Mohammadi et al. [18] synthesized carboxylated chitosan modified with ferromagnetic nanoparticles for adsorptive removal of nitrate anions from aqueous solutions. The maximum amounts of adsorption onto prepared nanoparticles were obtained in acidic conditions with 2 g/L of adsorbent. Yazdi et al. [19] removed nitrate from aqueous media by functionalized chitosan–clinoptilolite nanocomposites successfully.

Recent studies have shown that zero-valent iron (Fe^0), especially in nanoscale form, may potentially be used for water remediation, due to its affinity for a large number of contaminants, large specific surface area, and high surface reactivity [20–23]. Muradova et al. [20] investigated the removal of nitrate from groundwater by Fe/Cu bimetallic nanoparticles. They found that the rate of nitrate reduction increased by adding the ratio of copper particles to ZVI in two-part metal particles. Zou et al. [24] reported the excellent removal capacity of nZVI-based materials for various heavy metal ions. Sepehri et al. [25], removed nitrate (up to 84%) from aqueous solution by zero-valent iron nanoparticles reinforced with natural zeolite. Furthermore, the adsorption of some contaminants including amido black dye (up to 88% removal), ibuprofen (92%), ametryn (88%), propranolol drug residue (90%), pantoprazole drug residue (89%), secbumeton herbicide (90%), β-estradiol (82%), atrazine herbicide(95%), cyanazine (80%) onto iron nanocomposite material as adsorbent has been investigated by Ali et al. [26–34].

Titanium dioxide is a nontoxic material that has been applied in environmental treatments such as water and air disinfection because of relatively low price, corrosion resistance and its unique properties such as strong photocatalytic activity and high physical and chemical stability [35–38]. Titanium dioxide nanoparticles have been used to photocatalytic and adsorption removal of some pollutants [36, 39–48], but to the best of our knowledge, any research focused on removal of nitrate from water by adsorption on magnetized titanium dioxide nanoparticles and its comparison with unmodified TiO_2 nanoparticles has not yet been reported. The main aim of this study was to investigate the nitrate removal efficiency of TiO_2 nano-particles grafted with nZVI.

Experimental

Materials

Nano-TiO_2 powder (anatase-phase crystal structure with average particle size of about 25 nm) was supplied by Nanolin, Germany. Potassium nitrate (99%), ferric trichloride ($FeCl_3{\cdot}6H_2O$) with 99% purity, molecular mass 270.33 g/mol and density of 1.82 g/cm^3, sodium borohydride ($NaBH_4$) with a purity of 99%, molecular weight 37.83 g/mol and density of 0.0005 g/cm^3 and ethanol (≥ 99% purity) from Merck, Germany were used.

Preparation of TiO_2/nZVI nano-adsorbent

nZVI was synthesized in an anaerobic chamber via the reduction of Fe^{3+} ions with sodium borohydride as a reducing agent according to the method described by Huang [49]. Briefly, FeCl3·6H_2O was dropped to $NaBH_4$ solution in a 1:2 volume ratio. The black nZVI was separated and rinsed with pure ethanol and vacuum dried for 90 min at 160 mbar. The reduction process occurs according to the following equation [49]:

$$2Fe\left(H_2O\right)_6^{3+} + 6BH_4^- + 6H_2O \rightarrow 2Fe^0 + 6B(OH)_3 + 21H_2 \quad (1)$$

TiO_2/nZVI nanocomposite was prepared according to Petala et al. [37] method, during two stages: wet impregnation and then reduction with sodium borohydride. For this purpose, 0.2 g ferric trichloride was dissolved in 7 mL of pure ethanol and 0.4 g TiO_2 was added to this solution until saturation. Solvent evaporation was performed by heating in a hot water bath at 70 °C for 20 min. For reduction of Fe^{3+} to Fe^0, a reducing solution (containing 0.2 g sodium borohydride in 7 mL of deionized water) was added to the solution as dropwise. The mixture was kept stationary for 30 min until deposition and then centrifuged at 15,000 rpm for 15 min. Finally, the solid phase was rinsed and vacuum dried. All of [TiO_2]:[nZVI] ratios (0, 0.25, 0.5, 1, 2.5, 5 and 7), were produced in the same way. For this purpose, calculated mass amounts of TiO_2 were added to ferric trichloride solution. [Fe^{3+}]:[BH_4^-] ratio was kept constant.

Adsorption experiments

Adsorption experiments were conducted discontinuously to evaluate the nitrate adsorption efficiency. Certain concentrations of nitrate at specific contact times and pHs were subjected to different amounts of adsorbent, based on the relevant experiments design. Aqueous nitrate solution was stirred on a magnetic stirrer at 1000 rpm to allow the transfer of the pollutant onto the adsorbent. The main part of the magnetic adsorbent was separated from the solution using a magnet and the remainder was separated by centrifuge at 15,000 rpm for 15 min. The nitrate concentration was analyzed by spectrophotometry. The absorbance of the solutions was determined at $\lambda_{max} = 270$ nm using a UV–Vis spectrophotometer model 8454/4000 (USA).

The nitrate adsorption efficiency onTiO_2 and TiO_2/nZVI nanocomposite was obtained by the following formula:

$$\text{Adsorption efficiency} = \frac{C_0 - C_t}{C_0}, \quad (2)$$

where, C_0 is the initial nitrate concentration in the aqueous solution; C_t is the concentration of nitrate in the aqueous solution at t min.

Characterization of adsorbent

The morphology of unmodified and modified nanoparticles was evaluated using Cambridge S360 scanning electron microscope (SEM) equipped with an Oxford EDX. All images were taken with an operating voltage 30 kV and 200, 500, 1000 and 2000 magnifications. All the specimens were sputter-coated with gold in a Quorum sputter coater model Q 150R ES. A closer look at the shape, size, and arrangement of the nanostructure adsorbent was carried out by Philips transmission electron microscope (TEM) model CM120. The X-ray diffraction analysis(XRD) was performed at an angular range of 5°–70° (2θ) with a step size of $2\theta = 0.02°$ in Philips Analytical X-Ray diffractometer model X' Pert PW 3040/60 using a Cu K_α radiation ($\lambda = 1.5406$ nm), 40 kV, and 30 mA. The diffractometer was equipped with 1° divergence slit and a 0.1 mm receiving slit. Fourier transform infrared spectroscopy (FTIR) was carried out by the Thermo Nicolet apparatus model Avatar 370, made in USA. All the peaks were obtained in the range of 4000–400 cm^{-1} for modified and unmodified nano-adsorbents. Magnetization of the prepared nanocomposite (TiO_2/nZVI) was studied at room temperature using vibration sampling magnetometer (VSM) model 7400 (USA). This device is able to measure the magnetic properties of samples with an accuracy of 1×10^{-7} emu.

Regeneration and reusability of adsorbent

To evaluate the possibility of recycling the adsorbent, regeneration process of TiO_2/nZVI nanocomposites was conducted. A 0.01 M NaOH solution was used as adsorbent recovery solution. TiO_2/nZVI nanocomposites, previously saturated with nitrate, were agitated with NaOH solution for 3 h and followed by ultrasonication for 5 min to desorb the nitrate from them. Adsorbents were separated by centrifuge, and then washed by deionized water for 5 min. The denitrification performance of the regenerated adsorbent was measured in a new adsorption experiment. This adsorption–desorption cycle was repeated five times to test the reusability of the adsorbents [19, 50, 51].

Statistical analysis

Response surface method (RSM), central composite design(CCD) type was used for designing of experiments, analyzing resulted data and determining the influence of three factors "contact time", "pH" and "adsorbent dosage" with three levels for each one,on "adsorption efficiency" response. The levels of factors have been selected according to the preliminary tests. Design expert software version 10 was used for analysis of variance (ANOVA). The 0.05 significance level was used. The optimal value for each of the three parameters was determined according to the obtained responses. Factors under study along with their levels are summarized in Table 1.

Table 1 Factors under study along with their levels

Factor	Level	
	Low	High
A: Contact time (min)	60	210
B: pH	4	10
C: Adsorbent dosage (g/L)	0.5	1.5

Results and discussion

Morphological properties

SEM micrographs of titanium dioxide nanoparticles and their modified form are shown in Fig. 1a–d. The micrographs, taken from the surface of samples, illustrate that the particles are largely spherical and the modified particles are slightly larger than unmodified particles.

The larger size of TiO_2/nZVI nanoparticles (up to 70 nm) indicates the proper integration of TiO_2 nanoparticles with the modifier factor. As it is seen, the resulting nanocomposites are spherical with no agglomeration between particles.

TEM images taken from TiO_2/nZVI magnetic nanoparticles are shown in Fig. 1e, f. In the prepared TiO_2/nZVI nanocomposite structure, the coated core is visible that suggesting a good combination of TiO_2 nanoparticles with nZVI. Based on TEM results, the size of prepared magnetic nanoparticles was below 100 nm.

Structural properties

The element composition of the synthesized materials was identified by an energy-dispersive X-ray spectroscopy system (EDX) coupled to the SEM. EDX analysis of nanocomposites (Fig. 11), confirmed the presence of titanium, iron, oxygen and chlorine elements in the composition of the compound. The presence of some oxygen (33.37%) in the composition is not surprising, since the occurrence of partial oxidation is inevitable.

X-ray diffraction patterns related to TiO_2 nanoparticles and TiO_2/nZVI nanocomposites at $2\theta = 5°–70°$ are

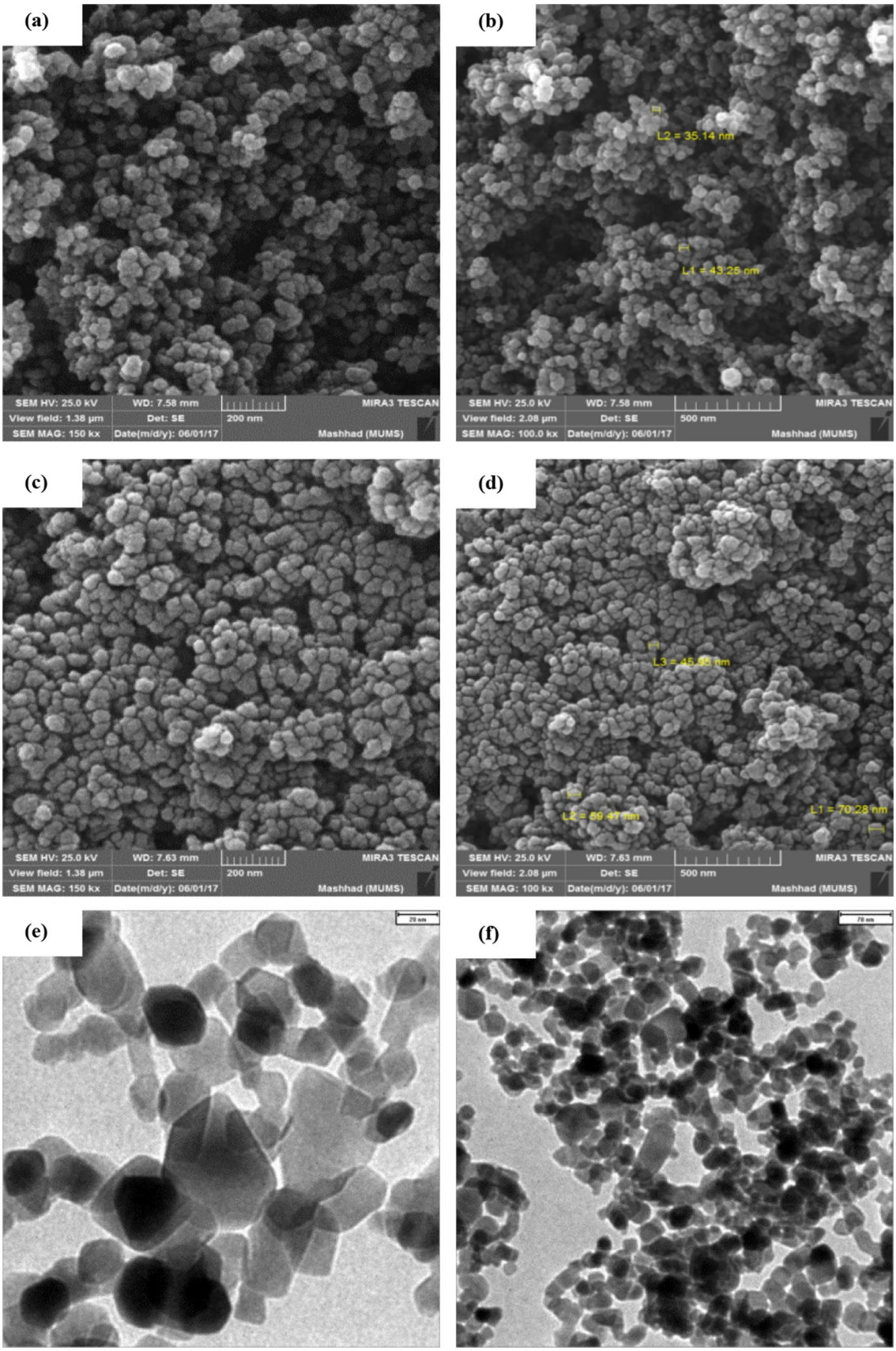

Fig. 1 **a**, **b** SEM images of titanium dioxide nanoparticle; **c**, **d** SEM images of TiO_2/nZVI nanocomposites; **e**, **f** TEM images of TiO_2/nZVI nanocomposites

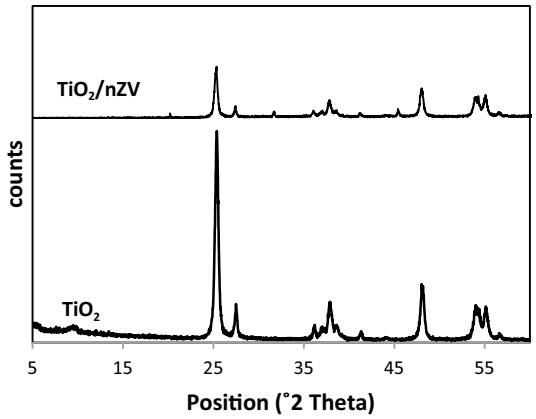

Fig. 2 X-ray diffraction patterns of TiO_2 and TiO_2/nZVI nanoparticles

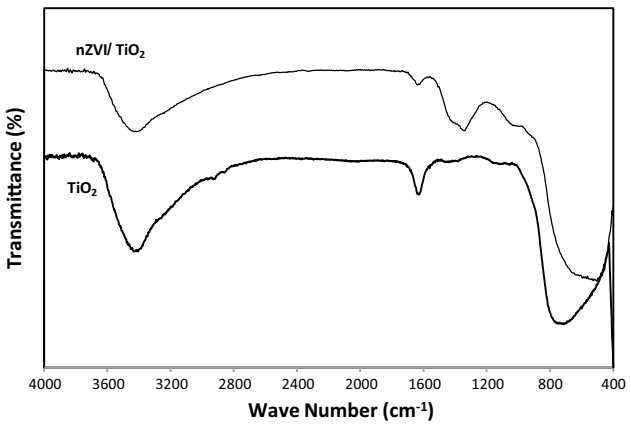

Fig. 3 FTIR spectra of TiO_2 and TiO_2/nZVI nanoparticles

shown in Fig. 2. As it is seen, TiO_2 exhibits a sharp peak at $2\theta = 25.402°$ corresponding to the plane spacing (d-spacing) of 0.351 nm [35]. The X-ray diffraction pattern of the magnetic nanocomposite has the same pattern as for TiO_2, with two excessive peaks in $2\theta = 31.8°$ and $2\theta = 44.9°$ which indicate the presence of Fe in the composition [38, 52]. The peak in $2\theta = 25°$ can correspond to the presence of TiO_2 and FeOOH in the nanocomposites [33]. Observed peak in $2\theta = 31.8°$ is related to the presence of iron oxide (FeO) and the peak in $2\theta = 44.9°$ indicating the presence of iron zero-valent crystalline phase [25, 53].

Fourier transform infrared radiation (FTIR) technique is used to understand the adsorption mechanism [11]. A comparison between the FTIR spectrums of TiO_2 and its modified form are shown in Fig. 3. In the nano-TiO_2 spectrum, a strong and broad absorption band at 3430.52 cm^{-1} shows a large amount of –OH at the nano-TiO_2 surface. Absorption band at 1629.16 cm^{-1} is related to Ti–OH bending vibration and the absorption band at 713.06 cm^{-1} indicates the Ti–O–Ti tensile vibration [54, 55].

Comparison between FTIR spectra of TiO_2/nZVI nanocomposite with the spectra of TiO_2 nanoparticles shows that the surface modification has been occurred [56]. In the TiO_2/nZVI spectrum, the broad band at 3415.20 cm^{-1} is related to tensile vibrations of –OH which should be in the range of 3200–3500 cm^{-1}. The peaks at 1637.51 cm^{-1} and 3415.20 cm^{-1} are also indicative of the tensile vibrations of OH related to H_2O and α-FeOOH [53]. A shift in the absorption band of Ti–O tensile vibration from 713.06 cm^{-1} to 503.65 cm^{-1} indicates the Ti–O composition with other elements during the surface modification process [56].

Magnetic properties of TiO_2/nZVI nano-adsorbent

The magnetic behavior of diamagnetic materials, paramagnetics, ferromagnetics, etc., can be measured in different shapes of powder, solid, thin film, single crystal, liquid, etc., using VSM with drawing of a residual curve. A representative hysteresis loop of TiO_2/nZVI nanocomposites at ambient temperature and in the fields from − 20,000 to 20,000 Oersted is shown in Fig. 4. The obtained hysteresis loop, suggested a weak magnetic nature of prepared nanocomposites. The weak magnetism was most likely attributed to the existence of nonconductor TiO_2 along with nZVI and the weak magnetic nature of nZVI itself. As it is seen, the response of prepared nanocomposite to the applied magnetic field indicates a ferromagnetic behavior. As expected, the residual is very low and also has a magnetic saturation. The saturation magnetization of the TiO_2/nZVI nanocomposite was about 795.28 memu/g. Petala et al. [37] in their research on synthesis and characterization of nZVI/TiO_2 for photocatalytic removal of chromium VI from water, achieved a ferromagnetic response with maximum magnetic properties of 16.1 Am^2/kg at 5 K and 13.8 Am^2/kg at 300 K without reaching saturation at any temperature. Lu et al. [38] reported a magnetic property of 1320 memu/g for Rectorite/TiO_2/Fe_3O_4 composites.

Optimization of factors

To determine the optimal nitrate removal conditions, the effect of contact time (60–210 min), pH (4–10) and adsorbent dosage (0.5–1.5 g/L) were studied. For this reason, the specific concentration of the contaminant, under controlled pH conditions was contacted with different amounts of adsorbent during certain contact times based on the design of experiments.

Effect of contact time

The effect of contact time on nitrate adsorption efficiency by TiO_2 and TiO_2/nZVI nanoparticles are shown in Fig. 5a, b.

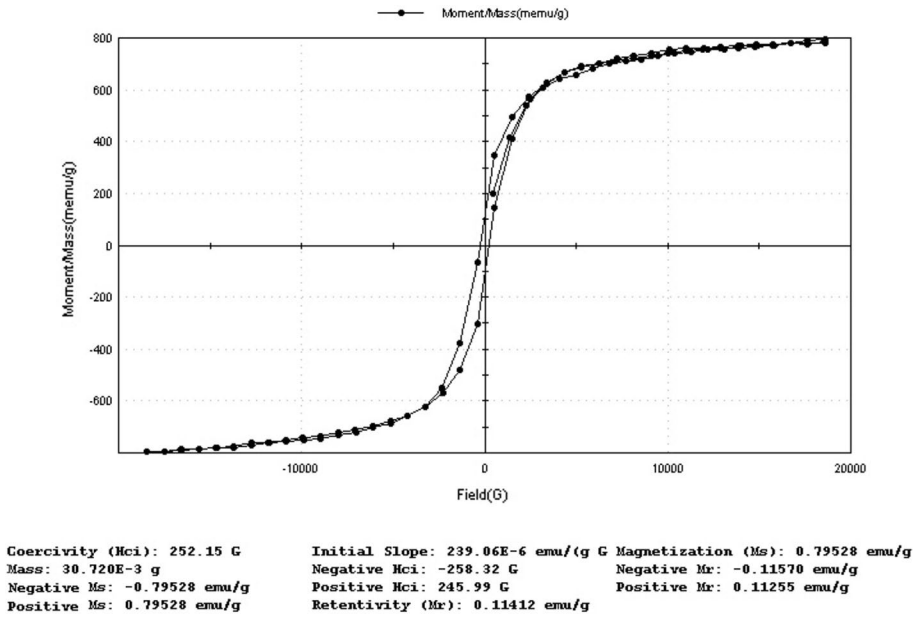

Fig. 4 Magnetic property of TiO_2/nZVI nanocomposite

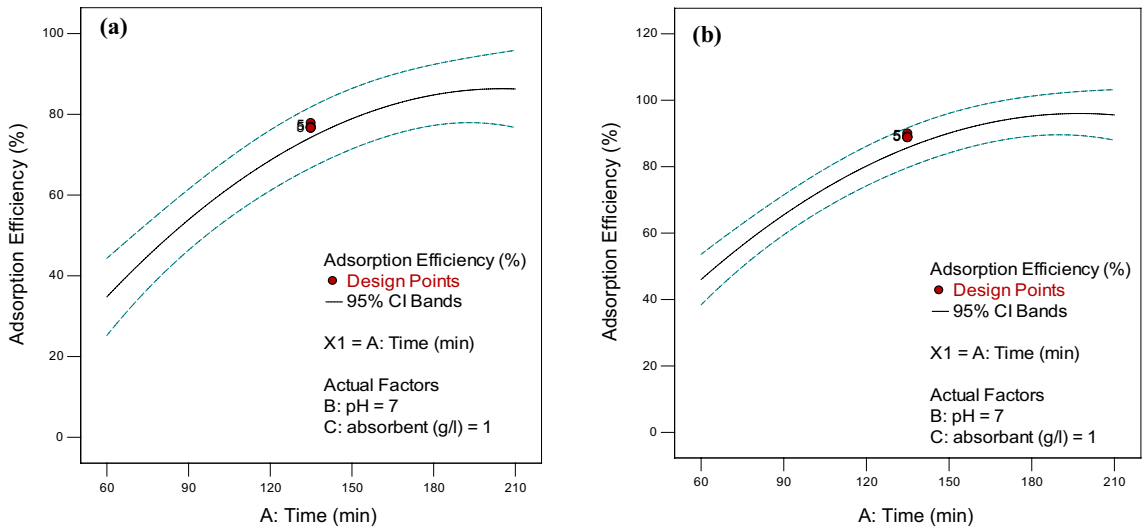

Fig. 5 Effect of contact time on nitrate adsorption by: **a** TiO_2 nanoparticles, **b** TiO_2/nZVI nanocomposites

As it can be seen, increasing the contact time has improved the efficiency of nitrate adsorption by the adsorbent. The main reason for increasing the amount of adsorption over time is increasing the collision chance of nitrate ions with active sites on the adsorbent. The major part of removal by unmodified TiO_2 nanoparticles occurred in the first 150 min, and by approaching to equilibrium, the amount of adsorption had no considerable progress. The maximum adsorption on unmodified TiO_2 nanoparticles was 82.9406% at 210 min. With increasing the contact time from 210 to 240 min, no further increase in adsorption efficiency occurred; this is due to adsorbent saturation over time. Bhatnagar et al. [2] had obtained the same result for removal of nitrate from water through adsorption on alumina nanoparticles. They observed that the adsorption process reached equilibrium within 60 min. Comparison of the obtained results showed that the maximum adsorption by modified TiO_2 was about 14.65% higher than the unmodified nanoparticle; this is due to the increased adsorbent surface and the high ability of zero-valent iron nanoparticles integrated with TiO_2 for removal of pollutants [20, 25, 57]. The obtained result matches the report by Muradova et al. [20] on the nitrate elimination from aqueous solution by nZVI/Cu nanoparticles. They also observed more reduction in concentration of nitrate at the beginning and in contact times more than 60 min, the concentration changes were little.

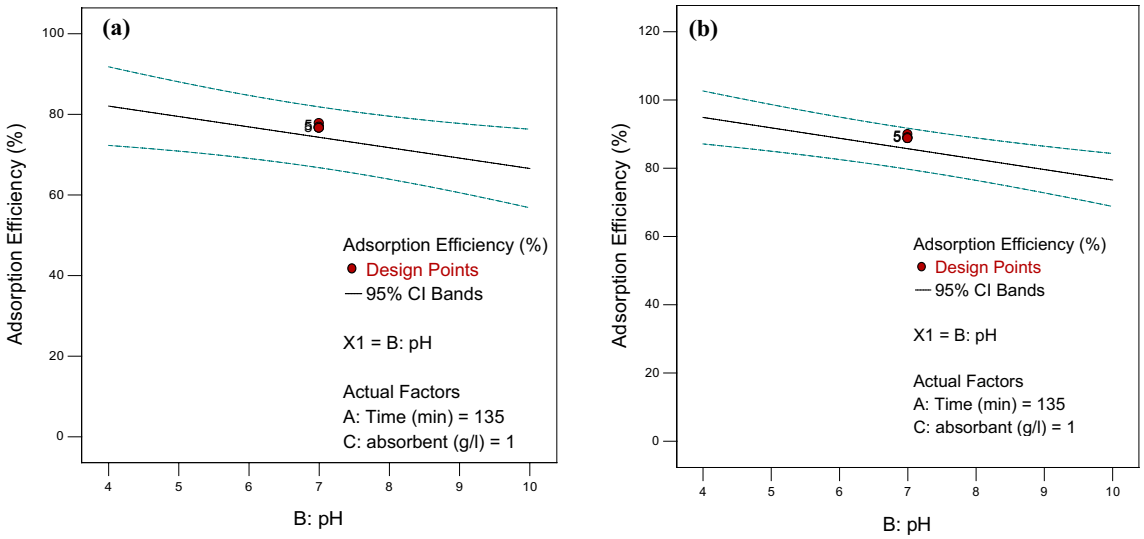

Fig. 6 Effect of pH on nitrate adsorption by: **a** TiO_2 nanoparticles, **b** TiO_2/nZVI nanocomposites

Effect of pH value

Figure 6a, b shows the effect of pH on nitrate removal efficiency by nano-TiO_2 and TiO_2/nZVI nanocomposites. The role of pH is crucial, as it may influence both the reactivity with the pollutants and the actual composition of adsorbent. In acidic conditions, the adsorbent surface is protonated and has a higher positive charge. This causes electrostatic interactions between adsorbents and negative charged ions in the water. In alkaline conditions, the surface of adsorbent has a negative charge and the interaction between adsorbent and positive ions will increase [58]. We found that the nitrate removal efficiencies decreased with increasing pH value. The adsorption mechanism was strong electrostatic interaction between H^+ ions that had been increased positive charges on adsorbent surface and negative charged nitrate ions. In high pHs because of the competition between OH^- ions present in alkaline environment and anionic nitrate for sit on adsorbent active sites, nitrate removal was decreased. The highest adsorption efficiencies on nano-TiO_2 and TiO_2/nZVI nanocomposite were 82.9406% and 95.092% at pH 4, respectively. The maximum adsorption efficiency by TiO_2/nZVI has indicated an improvement equal to 14.45% in the presence of nZVI. Bhatnagar et al. [2] also observed that the adsorption efficiency of nitrate by nano-alumina was increased in pH range from 3 to 4.4; it then decreased along with an increase in pH. Xie and Gao [39] also had used TiO_2 nanoparticles to remove heavy metals from water. They had observed less absorption efficiency for metal cations in low pHs because of the competition between H^+ and positively metal ions; Conversely, at high pHs, the adsorbent was deprotonated and was more likely to absorb cationic metals. Ai et al. [59] have reported that the sorption of U(VI) towards graphene oxide was primarily influenced by the pH values of the aqueous solution, and its adsorption performance was strongest at high pH levels. The adsorption mechanism was strong electrostatic interaction between the uranyl ion and the negative charged O atoms of the oxygen-containing functional groups, which were the main adsorption sites also. Based on their opinion, in addition to the pH influence, an increase in functional groups and negative charges on the GO surface can improve the adsorption ability towards uranyl ions.

Effect of adsorbent dosage

Effect of adsorbent dosage on the adsorption efficiency is shown in Fig. 7a, b. As it is clear from this figure, the efficiency of nitrate adsorption initially has improved by increasing the amount of adsorbent and then remained constant. This result is similar to what proposed by Ali et al. in their studies on molecular uptake of Congo red dye from water on iron composite nano-particles [60] and fast removal of fluoride from water by iron nano-impregnated adsorbent [61].

When using unmodified TiO_2, with an increase in the amount of adsorbent from 0.3 to 1 g/L, the adsorption efficiency increased from 14.285 to 82.637% (approximately 478.5% improvement) while with increasing the adsorbent from 1 to 1.5 g/L, only 0.36% increase in removal efficiency was observed. Therefore, increasing the amount of adsorbent to more than 1 g/L will not increase the adsorption efficiency significantly. The maximum nitrate removal efficiency with TiO_2/nZVI nanocomposites was 95.092% using 1.5 g/L adsorbent, which is 14.65% higher than that of the unmodified TiO_2 with the same adsorbent dosage. We attribute these

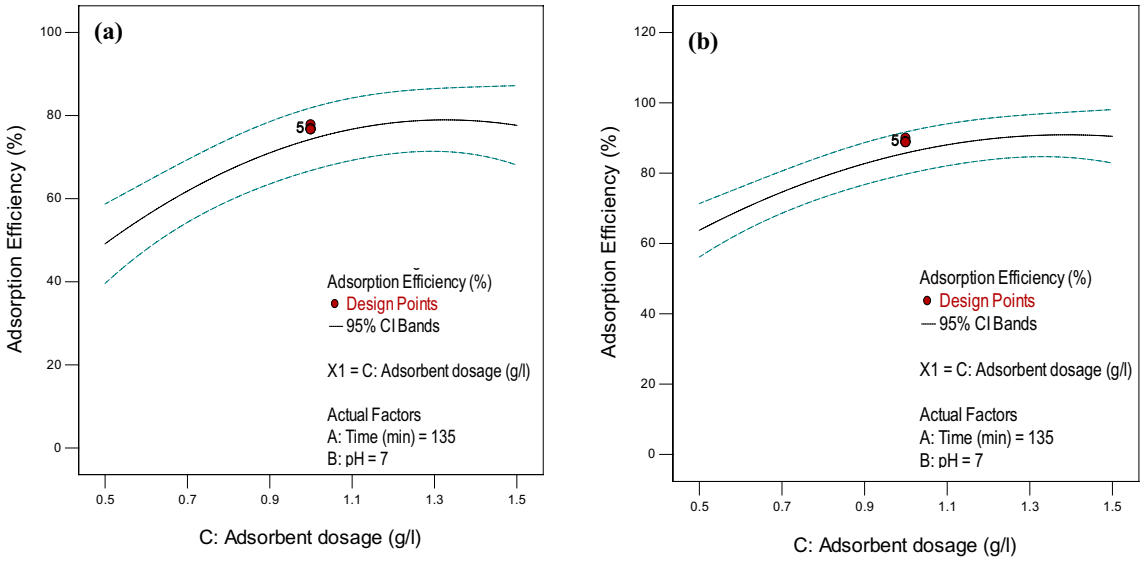

Fig. 7 Effect of adsorbent dosage on nitrate adsorption by: **a** TiO_2 nanoparticles, **b** TiO_2/nZVI nanocomposites

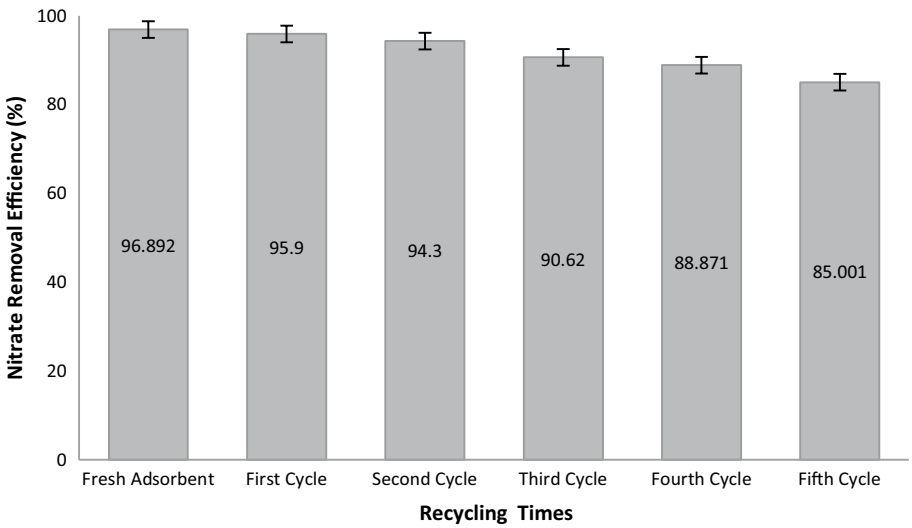

Fig. 8 Nitrate removal efficiency of TiO_2/nZVI adsorbent (at optimal conditions) over five regeneration cycles

results to good surface characteristics of prepared composite nano-adsorbent and its suitable interaction with nitrate molecules. Consequently, grafting the TiO_2 nanoparticles with nZVI has improved the adsorption capability of the adsorbent. Statistical analysis, also showed that the influence of adsorbent dosage on removal efficiency was significant ($P < 0.05$). The high performance of nano-zero-valent iron to remove various pollutants had been reported previously [24, 25, 37, 62].

Regeneration and reusability of modified TiO_2

The regeneration of an adsorbent is one of the most important aspects for an economical adsorption process. Therefore, to reduce costs and waste production, regeneration tests for recycling TiO_2/nZVI nanocomposites were conducted and the results are shown in the Fig. 8. Results indicated that the adsorption efficiency decreased after each cycle of adsorption–regeneration slightly and there was no significant difference during five adsorption–regeneration cycles. The first-time regenerated TiO_2/nZVI nanocomposites could remove 95.9% of nitrate (only 0.992% less than the fresh adsorbent) and 85.001% after five time regeneration. Therefore, the obtained results confirm that the majority of adsorbent can recycle. Qin et al. [63] in their study on mesoporous TiO_2–SiO_2 adsorbent for ultra-deep desulfurization of organic-S had observed that the first-time regenerated adsorbent could recover 99% of the breakthrough capacity as

Table 2 Predicted and experimental optimal conditions for nitrate removal by TiO_2/nZVI

Contact time (min)	pH	Adsorbent (g/L)	Adsorption efficiency (%): predicted	Adsorption efficiency (%): from experiment	Error (%)
150.091	4.185	0.982	98.226	96.892	1.358

compared to a fresh adsorbent and after the fifth regeneration, it could recover 94.5%.

Statistical results

Analysis of the results by Design Expert software showed that the quadratic model is statistically well matched to the obtained data for nitrate adsorption onto the TiO_2 nanoparticles before and after grafting with nZVI. The obtained equations for nitrate adsorption efficiency by TiO_2 nanoparticles based on the coding and real factors, respectively, were:

$$\text{Adsorption efficiency (\%)} = +74.31 + 25.75 * A - 7.74 * B + 14.25 * C - 13.77 * A^2 - 10.92 * C^2 \quad (3)$$

$$\text{Adsorption efficiency (\%)} = -70.77102 + 1.00435 * \text{Time (min)} - 2.57911 * \text{pH} + 115.85303 * \text{adsorbent (g/l)} - 2.44834E - 003 * \text{Time (min)}^2 - 43.68022 * \text{adsorbent (g/l)}^2 \quad (4)$$

The obtained equations for nitrate adsorption efficiency by TiO_2/nZVI nanocomposites based on the coding and real factors, respectively, were:

$$\text{Adsorption efficiency (\%)} = +85.74 + 24.78 * A - 9.16 * B + 13.36 * C - 14.93 * A^2 - 8.62 * C^2 \quad (5)$$

$$\text{Adsorption efficiency (\%)} = -47.08448 + 1.04717 * \text{Time (min)} - 3.05371 * \text{pH} + 95.69313 * \text{adsorbent (g/l)} - 2.65464E - 003 * \text{Time (min)}^2 - 34.48179 * \text{adsorbent (g/l)}^2 \quad (6)$$

Design Expert software has been used to determine the optimal removal conditions within the tested range. Predicted and experimental optimum conditions for nitrate removal by TiO_2/nZVI along with the maximum adsorption value are presented in Table 2.

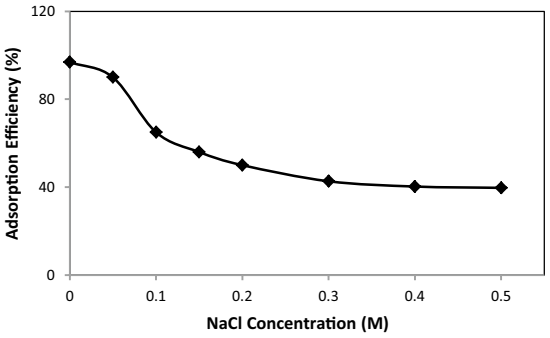

Fig. 9 Effect of ionic strength on nitrate adsorption efficiency

Effect of ionic strength

To study the effect of ionic strength on nitrate removal efficiency, the salt content of the feed solution was adjusted for the optimized conditions (adsorbent dosage 0.982 g/L, pH 4.185 and the contact time 150.091 min). Obtained results illustrated that the nitrate removal decreased as the ionic strength increased (Fig. 9). This removal decrease may be because of the competitive adsorption among NO_3^- and interfering Cl^- ions toward the adsorbent. Similar findings were reported by Kim and Zazouli in their works on nitrate adsorption by nZVI [22, 64]. Ali et al. [33] also reported the same result for atrazine herbicide adsorption onto the iron nanocomposite.

Effect of different TiO_2:nZVI ratios

The efficiencies of nitrate removal by TiO_2, nZVI and TiO_2/nZVI were studied at determined optimized conditions. A removal efficiency of 78.9% and 65.73% were able to be achieved using TiO_2 and nZVI nanoparticles alone, while the nitrate removal was increased up to 96.892% using TiO_2/nZVI nanocomposites. Figure 10 shows the nitrate removal efficiencies with different ratios of TiO_2/nZVI adsorbents at constant nitrate concentration of 200 mg/L and optimum conditions. On the basis of obtained results, the effect of grafting the TiO_2 nanoparticles with nZVI on nitrate removal efficiency is apparent. It can be seen that TiO_2:nZVI ratio has strongly influenced the nitrate removal performance of the adsorbent. By increasing the amount of TiO_2 in the adsorbent composition, its performance was significantly improved. However, increasing the TiO_2:nZVI ratio to more than 7 times, reduced the efficiency of the adsorbent.

The major problem for Fe^0 application as an adsorbent is its high agglomeration and the formation of a surface oxide layer and that for TiO_2 is the limit of the efficiency due to the recombination phenomenon [49]. Our results indicated that grafting TiO_2 with ZVI nanoparticles has overcome these problems as well as to improve their performance. Huang et al. [49] in a similar study, reported that the efficiency of

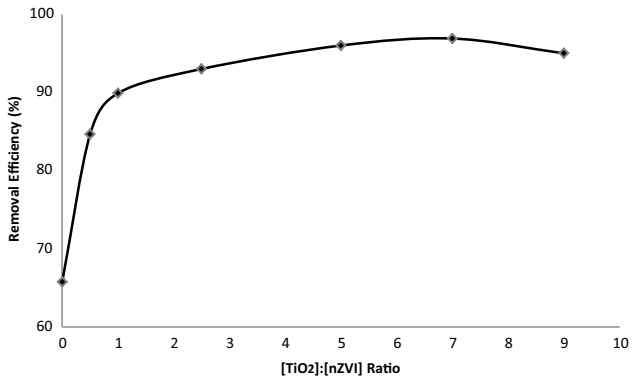

Fig. 10 Effect of different TiO_2/nZVI ratios on nitrate adsorption efficiency

TiO_2/Fe^0 composite on azo dye reduction is much more than microscale and nanoscale Fe^0 and TiO_2 particles. Ulucan-Altuntas et al. [65] in their study on the effect of activated carbon/nZVI ratio on removal of nickel ion from water, indicated that the adsorption capacity was increased from 125 and 820 mg/g for activated carbon and nZVI, respectively, to 1190 mg/g for 50% AC/nZVI nanocomposite.

Conclusions

The developed functionalized TiO_2/nZVI nanocomposites were effective for nitrate elimination from water and had a good reusability. Denitrification of nitrate by nanoscale ZVI particles includes the direct reduction by metallic iron and indirect reduction by the iron corrosion product, hydrogen; but with respect to the using of TiO_2 in the composite structure, it seems that adsorption has been the main mechanism for nitrate removal. On the basis of SEM and TEM morphological analyses, the prepared nanocomposites were spherical with no agglomeration between particles and the coated core was visible. In VSM study, the response of prepared nanocomposite to the applied magnetic field indicated a ferromagnetic behavior. This magnetic property of the particles makes it easier to separate them from the solution. Comparison of the obtained results showed that the maximum adsorption by modified TiO_2 was about 14.65% higher than the unmodified nanoparticles. Therefore, the combination of nano-TiO_2 with nZVI would greatly improve its nitrate adsorption efficiency. The optimal conditions predicted for a maximum nitrate separation of 98.226% by TiO_2/nZVI nanocomposites were: adsorbent dosage 0.982 g/L, pH 4.185 and the contact time 150.091 min. Regeneration process was carried out with NaOH and proven it was an effective agent in the discharge of nitrate.

Acknowledgements The authors sincerely thank the officials at Islamic Azad University, Quchan Branch, for their financial support and the provision of laboratory equipment.

Open Access This article is distributed under the terms of the Creative Commons Attribution 4.0 International License (http://creativecommons.org/licenses/by/4.0/), which permits unrestricted use, distribution, and reproduction in any medium, provided you give appropriate credit to the original author(s) and the source, provide a link to the Creative Commons license, and indicate if changes were made.

Appendix

See Fig. 11.

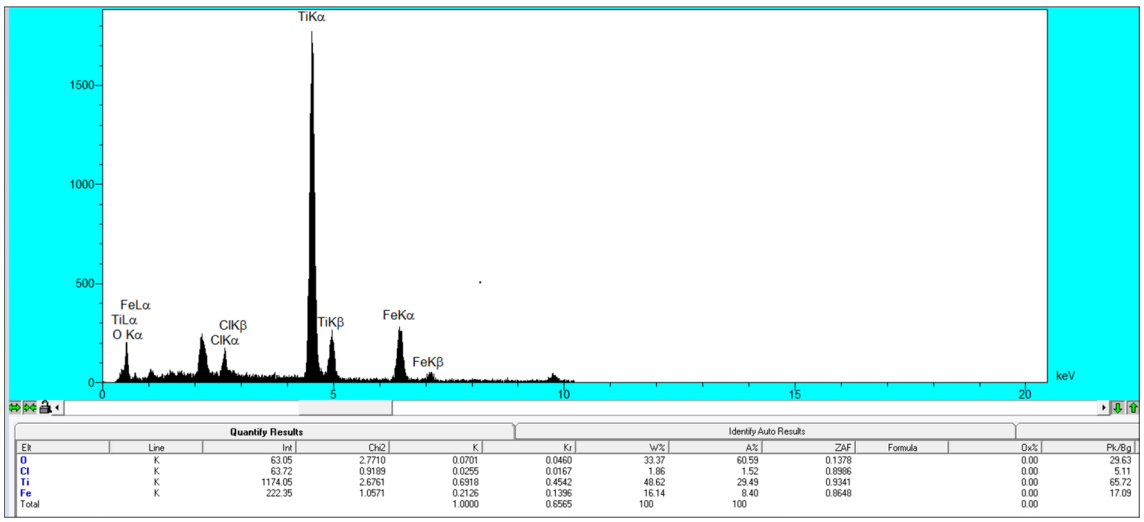

Fig. 11 EDX analysis of TiO_2/nZVI nanocomposites

References

1. Samatya S, Kabay N, Yüksel Ü, Arda M, Yüksel M (2006) Removal of nitrate from aqueous solution by nitrate selective ion exchange resins. React Funct Polym 66(11):1206–1214
2. Bhatnagar A, Kumar E, Sillanpää M (2010) Nitrate removal from water by nano-alumina: characterization and sorption studies. Chem Eng J 163(3):317–323
3. Gu P, Zhang S, Li X, Wang X, Wen T, Jehan R, Alsaedi A, Hayat T, Wang X (2018) Recent advances in layered double hydroxide-based nanomaterials for the removal of radionuclides from aqueous solution. Environ Pollut 240:493–505
4. Jensen VB, Darby JL, Seidel C, Gorman C (2014) Nitrate in potable water supplies: alternative management strategies. Crit Rev Environ Sci Technol 44(20):2203–2286
5. Liu G, You S, Ma M, Huang H, Ren N (2016) Removal of nitrate by photocatalytic denitrification using nonlinear optical material. Environ Sci Technol 50(20):11218–11225
6. Gupta VK, Ali I (2012) Environmental water: advances in treatment, remediation and recycling. Newnes, Oxford
7. Ali I (2012) New generation adsorbents for water treatment. Chem Rev 112(10):5073–5091
8. Ali I (2014) Water treatment by adsorption columns: evaluation at ground level. Sep Purif Rev 43(3):175–205
9. Ali I, Gupta V (2006) Advances in water treatment by adsorption technology. Nat Protoc 1(6):2661
10. Wang X, Liu Y, Pang H, Yu S, Ai Y, Ma X, Song G, Hayat T, Alsaedi A, Wang X (2018) Effect of graphene oxide surface modification on the elimination of Co (II) from aqueous solutions. Chem Eng J 344:380–390
11. Li J, Wang X, Zhao G, Chen C, Chai Z, Alsaedi A, Hayat T, Wang X (2018) Metal–organic framework-based materials: superior adsorbents for the capture of toxic and radioactive metal ions. Chem Soc Rev 47(7):2322–2356
12. Li X, Liu Y, Zhang C, Wen T, Zhuang L, Wang X, Song G, Chen D, Ai Y, Hayat T (2018) Porous Fe_2O_3 microcubes derived from metal organic frameworks for efficient elimination of organic pollutants and heavy metal ions. Chem Eng J 336:241–252
13. Zhao G, Huang X, Tang Z, Huang Q, Niu F, Wang X-K (2018) Polymer-based nanocomposites for heavy metal ions removal from aqueous solution: a review. Polym Chem 9(26):3562–3582
14. Gupta V, Ali I (2002) Encyclopedia of surface and colloid science. Marcel Dekker, New York, pp 136–166
15. Khezri SM, Bloorchian AA (2009) Titanium dioxide extraction from paint sludge of auttomotive industry case study: paint sludge of saipa shop. Environ Eng Manag J 8(1):141–145
16. Yu S, Wang X, Pang H, Zhang R, Song W, Fu D, Hayat T, Wang X (2017) Boron nitride-based materials for the removal of pollutants from aqueous solutions: a review. Chem Eng J 333:343–360
17. Farasati M, Nasab SB, Moazed H, Haghighifard NJ, Koupai JA, Seyedian M (2011) Nitrate removal from contaminated waters by using anion exchanger *Phragmites australis* nanoparticles. Water Wastewater 1:34–42
18. Mohammadi E, Daraei H, Ghanbari R, Athar SD, Zandsalimi Y, Ziaee A, Maleki A, Yetilmezsoy K (2019) Synthesis of carboxylated chitosan modified with ferromagnetic nanoparticles for adsorptive removal of fluoride, nitrate, and phosphate anions from aqueous solutions. J Mol Liq 273:116–124
19. Yazdi F, Anbia M, Salehi S (2019) Characterization of functionalized chitosan-clinoptilolite nanocomposites for nitrate removal from aqueous media. Int J Biol Macromol 130:545–555
20. Muradova GG, Gadjieva SR, Di Palma L, Vilardi G (2016) Nitrates removal by bimetallic nanoparticles in water. Chem Eng Trans 47:205–210
21. Mukherjee R, Kumar R, Sinha A, Lama Y, Saha AK (2016) A review on synthesis, characterization, and applications of nano zero valent iron (nZVI) for environmental remediation. Crit Rev Environ Sci Technol 46(5):443–466
22. Kim D-G, Hwang Y-H, Shin H-S, Ko S-O (2016) Kinetics of nitrate adsorption and reduction by nano-scale zero valent iron (NZVI): effect of ionic strength and initial pH. J Civil Eng 20(1):175–187
23. Zhu F, Li L, Ren W, Deng X, Liu T (2017) Effect of pH, temperature, humic acid and coexisting anions on reduction of Cr (VI) in the soil leachate by nZVI/Ni bimetal material. Environ Pollut 227:444–450
24. Zou Y, Wang X, Khan A, Wang P, Liu Y, Alsaedi A, Hayat T, Wang X (2016) Environmental remediation and application of nanoscale zero-valent iron and its composites for the removal of heavy metal ions: a review. Environ Sci Technol 50(14):7290–7304
25. Sepehri S, Heidarpour M, Abedi-Koupai J (2014) Nitrate removal from aqueous solution using natural zeolite-supported zero-valent iron nanoparticles. Soil Water Res 9(4):224–232
26. Ali I, Alharbi OM, Alothman ZA, Badjah AY, Alwarthan A (2018) Artificial neural network modelling of amido black dye sorption on iron composite nano material: kinetics and thermodynamics studies. J Mol Liq 250:1–8
27. Ali I, Al-Othman ZA, Alwarthan A (2016) Synthesis of composite iron nano adsorbent and removal of ibuprofen drug residue from water. J Mol Liq 219:858–864
28. Ali I, Al-Othman ZA, Alwarthan A (2016) Green synthesis of functionalized iron nano particles and molecular liquid phase adsorption of ametryn from water. J Mol Liq 221:1168–1174
29. Ali I, Alothman ZA, Alwarthan A (2017) Uptake of propranolol on ionic liquid iron nanocomposite adsorbent: kinetic, thermodynamics and mechanism of adsorption. J Mol Liq 236:205–213
30. Ali I, Al-Othman ZA, Alharbi OM (2016) Uptake of pantoprazole drug residue from water using novel synthesized composite iron nano adsorbent. J Mol Liq 218:465–472
31. Ali I, Al-Othman ZA, Al-Warthan A (2016) Removal of secbumeton herbicide from water on composite nanoadsorbent. Desalination Water Treat 57(22):10409–10421
32. Ali I, Alothman ZA, Alwarthan A (2017) Supra molecular mechanism of the removal of 17-β-estradiol endocrine disturbing pollutant from water on functionalized iron nano particles. J Mol Liq 241:123–129
33. Ali I, Alothman Z, Al-Warthan A (2016) Sorption, kinetics and thermodynamics studies of atrazine herbicide removal from water using iron nano-composite material. Int J Environ Sci Technol 13(2):733–742
34. Ali I, Alharbi OM, Alothman ZA, Alwarthan A (2018) Facile and eco-friendly synthesis of functionalized iron nanoparticles for cyanazine removal in water. Colloids Surf B Biointerfaces 171:606–613
35. Hejri Z, Seifkordi AA, Ahmadpour A, Zebarjad SM, Maskooki A (2013) Biodegradable starch/poly (vinyl alcohol) film reinforced with titanium dioxide nanoparticles. Int J Min Met Mater 20(10):1001–1011
36. Ghasemi Z, Seif A, Ahmadi TS, Zargar B, Rashidi F, Rouzbahani GM (2012) Thermodynamic and kinetic studies for the adsorption of Hg(II) by nano-TiO_2 from aqueous solution. Adv Powder Technol 23(2):148–156
37. Petala E, Baikousi M, Karakassides MA, Zoppellaro G, Filip J, Tuček J, Vasilopoulos KC, Pechoušek J, Zbořil R (2016) Synthesis, physical properties and application of the zero-valent iron/titanium dioxide heterocomposite having high activity for the sustainable photocatalytic removal of hexavalent chromium in water. Phys Chem Che Phys 18(15):10637–10646

38. Lu Y, Chang PR, Zheng P, Ma X (2014) Rectorite–TiO_2–Fe_3O_4 composites: assembly, characterization, adsorption and photodegradation. Chem Eng J 255:49–54
39. Xie X, Gao L (2009) Effect of crystal structure on adsorption behaviors of nanosized TiO_2 for heavy-metal cations. Curr Appl Phys 9(3):S185–S188
40. Visa M, Carcel RA, Andronic L, Duta A (2009) Advanced treatment of wastewater with methyl orange and heavy metals on TiO_2, fly ash and their mixtures. Catal Today 144(1):137–142
41. Parshetti GK, Doong R-a (2010) Dechlorination and photodegradation of trichloroethylene by Fe/TiO_2 nanocomposites in the presence of nickel ions under anoxic conditions. Appl Catal B Environ 100(1):116–123
42. Al-Rashdi B, Tizaoui C, Hilal N (2012) Copper removal from aqueous solutions using nano-scale diboron trioxide/titanium dioxide (B_2O_3/TiO_2) adsorbent. Chem Eng J 183:294–302
43. Parida K, Mishra KG, Dash SK (2012) Adsorption of toxic metal ion Cr(VI) from aqueous state by TiO_2-MCM-41: equilibrium and kinetic studies. J Hazard Mater 241:395–403
44. Jiang Y, Luo Y, Zhang F, Guo L, Ni L (2013) Equilibrium and kinetic studies of CI Basic Blue 41 adsorption onto N, F-codoped flower-like TiO_2 microspheres. Appl Surf Sci 273:448–456
45. Zhang N, Yang M-Q, Liu S, Sun Y, Xu Y-J (2015) Waltzing with the versatile platform of graphene to synthesize composite photocatalysts. Chem Rev 115(18):10307–10377
46. Zhang Y, Chen Z, Liu S, Xu Y-J (2013) Size effect induced activity enhancement and anti-photocorrosion of reduced graphene oxide/ZnO composites for degradation of organic dyes and reduction of Cr(VI) in water. Appl Catal B Environ 140:598–607
47. Lu K-Q, Xin X, Zhang N, Tang Z-R, Xu Y-J (2018) Photoredox catalysis over graphene aerogel-supported composites. J Mater Chem A Mater 6(11):4590–4604
48. Weng B, Lu K-Q, Tang Z, Chen HM, Xu Y-J (2018) Stabilizing ultrasmall Au clusters for enhanced photoredox catalysis. Nat Commun 9(1):1543
49. Huang C, Hsieh W-P, Pan JR, Chang S-M (2007) Characteristic of an innovative TiO_2/Fe^0 composite for treatment of azo dye. Sep Purif Technol 58(1):152–158
50. Sarkar K, Banerjee S, Kundu P (2012) Removal of anionic dye in acid solution by self crosslinked insoluble dendronized chitosan. Hydrol Curr Res 3(133):2
51. Dahri MK, Kooh MRR, Lim LB (2014) Water remediation using low cost adsorbent walnut shell for removal of malachite green: equilibrium, kinetics, thermodynamic and regeneration studies. J Environ Chem Eng 2(3):1434–1444
52. Zhang J, Hao Z, Zhang Z, Yang Y, Xu X (2010) Kinetics of nitrate reductive denitrification by nanoscale zero-valent iron. Process Saf Environ Prot 88(6):439–445
53. Liu A, Zhang W-x (2014) Fine structural features of nanoscale zero-valent iron characterized by spherical aberration corrected scanning transmission electron microscopy (Cs-STEM). Analyst 139(18):4512–4518
54. León A, Reuquen P, Garín C, Segura R, Vargas P, Zapata P, Orihuela PA (2017) FTIR and Raman characterization of TiO2 nanoparticles coated with polyethylene glycol as carrier for 2-methoxyestradiol. Appl Sci 7(1):49
55. Bagheri S, Shameli K, Abd Hamid SB (2012) Synthesis and characterization of anatase titanium dioxide nanoparticles using egg white solution via Sol-Gel method. J Chem 2013:1–5
56. Afkhami A, Bagheri H, Madrakian T (2011) Alumina nanoparticles grafted with functional groups as a new adsorbent in efficient removal of formaldehyde from water samples. Desalination 281:151–158
57. Pan JR, Huang C, Hsieh W-P, Wu B-J (2012) Reductive catalysis of novel TiO_2/Fe^0 composite under UV irradiation for nitrate removal from aqueous solution. Sep Purif Technol 84:52–55
58. Suriyaraj S, Vijayaraghavan T, Biji P, Selvakumar R (2014) Adsorption of fluoride from aqueous solution using different phases of microbially synthesized TiO_2 nanoparticles. J Environ Chem Eng 2(1):444–454
59. Ai Y, Liu Y, Lan W, Jin J, Xing J, Zou Y, Zhao C, Wang X (2018) The effect of pH on the U (VI) sorption on graphene oxide (GO): a theoretical study. Chem Eng J 343:460–466
60. Ali I, Al-Othman ZA, Alwarthan A (2016) Molecular uptake of congo red dye from water on iron composite nano particles. J Mol Liq 224:171–176
61. Ali I, Al-Othman ZA, Sanagi MM (2015) Green synthesis of iron nano-impregnated adsorbent for fast removal of fluoride from water. J Mol Liq 211:457–465
62. Li S, Wang W, Liang F, Zhang W-x (2017) Heavy metal removal using nanoscale zero-valent iron (nZVI): theory and application. J Hazard Mater 322:163–171
63. Qin B, Shen Y, Xu B, Zhu S, Li P, Liu Y (2018) Mesoporous TiO_2–SiO_2 adsorbent for ultra-deep desulfurization of organic-S at room temperature and atmospheric pressure. RSC Adv 8(14):7579–7587
64. Zazouli MA, Tilaki RAD, Safarpour M (2014) Modeling nitrate removal by nano-scaled zero-valent iron using response surface methodology. Health Scope 3(3):1–7
65. Ulucan-Altuntas K, Debik E, Gungor S (2018) Nano zero-valent iron supported on activated carbon: effect of AC/nZVI ratio on removal of nickel ion from water. Global Nest J 20(2):424–431

Publisher's Note Springer Nature remains neutral with regard to jurisdictional claims in published maps and institutional affiliations.